Charge Separation in Semicrystalline Polymeric Semiconductors by Photoexcitation: Is the Mechanism Intrinsic or Extrinsic?

Francis Paquin,[1] Gianluca Latini,[2,*] Maciej Sakowicz,[1] Paul-Ludovic Karsenti,[1] Linjun Wang,[3] David Beljonne,[3] Natalie Stingelin,[2] and Carlos Silva[1,†]

[1]*Département de physique and Regroupement québécois sur les matériaux de pointe, Université de Montréal, C.P. 6128, Succursale centre-ville, Montréal (Québec), H3C 3J7, Canada*

[2]*Department of Materials and Centre for Plastic Electronics, Imperial College London, South Kensington Campus, London SW7 2AZ, United Kingdom*

[3]*Chemistry of Novel Materials, University of Mons, Place du Parc 20, B-7000 Mons, Belgium*

(Received 31 January 2011; published 13 May 2011)

We probe charge photogeneration and subsequent recombination dynamics in neat regioregular poly(3-hexylthiophene) films over six decades in time by means of time-resolved photoluminescence spectroscopy. Exciton dissociation at 10 K occurs extrinsically at interfaces between molecularly ordered and disordered domains. Polaron pairs thus produced recombine by tunneling with distributed rates governed by the distribution of electron-hole radii. Quantum-chemical calculations suggest that hot-exciton dissociation at such interfaces results from a high charge-transfer character.

DOI: 10.1103/PhysRevLett.106.197401 PACS numbers: 78.55.Kz, 72.20.Jv, 78.47.jd, 78.66.Qn

Unraveling primary electronic processes in polymeric semiconductors opens a fundamental window to their materials physics. The steps to generate charge by optical absorption are currently the subject of wide interest [1]. Here, we focus on charge generation and recombination dynamics in *neat* regioregular poly(3-hexylthiophene) (P3HT). This semicrystalline polymer adopts π-stacked lamellar microstructures in the solid state [2], leading to two-dimensional electronic dispersion [3]. Crystallinity induced by molecular organization profoundly influences electronic properties, exemplified by the high yield (η) of apparently direct charge photogeneration. Whereas in general $\eta \ll 1\%$ in less organized polymeric semiconductors [4], various groups have reported η up to 30% over ultrafast time scales in P3HT films at 300 K [5–9]. However, photoemission spectroscopy measurements place the energy for free polaron generation $\sim$0.7 eV above the optical gap in neat P3HT [10]. Weak interchain electronic coupling in the lamellar architecture leads to a free-exciton bandwidth—the pure electronic bandwidth due to dispersion neglecting coupling to vibrations—that is well below this energy [11–13]. Thus, are charges indeed generated *intrinsically* (directly by photoexcitation due to the crystalline electronic structure) or *extrinsically* (due to a driving force for exciton dissociation)?

Charge photogeneration in neat P3HT has been studied previously by means of transient absorption spectroscopy [7,9], which measures directly the dynamics of nascent polarons. We implement time-resolved photoluminescence (PL) spectroscopy at 10 K to probe charge photogeneration and recombination dynamics. Our strategy is to exploit the intricate detail of electronic structure, structural relaxation, and correlated disorder afforded by the spectral band shape of the PL spectrum [12], over time scales where it is known that charge photogeneration is important. We probe the recombination environment via the band shape and decay dynamics of delayed PL from charge-pair recombination, which also probes the environment in which photogeneration occurs, since photoexcitations are frozen at 10 K. We find that charge generation occurs over subnanosecond time scales by dissociation of excitons created at interfaces between lamellar (aggregate) and poorly stacked (nonaggregate) domains, driven by energetic disorder. Thus, prompt charge photogeneration is an *extrinsic* process, and film microstructure determines the surface area and the energy landscape of interfaces between domains.

PL measurements were carried out with a 40-fs, 532-nm (2.33-eV) pulse train derived from an optical parametric amplifier (Light Conversion TOPAS), pumped by a Ti:sapphire laser system (KMLabs Dragon). Time-resolved PL spectra were measured with an optically triggered streak camera (Axis-Photonique, 6-ps instrument response). Alternatively, an intensified CCD camera (Princeton-Instruments PIMAX 1024HB) was used. P3HT films (Merck, $M_w = 47.8$ kg/mol, 150-nm thick) were spun from trichlorobenzene solution (6% wt).

In P3HT films, the PL spectrum is understood within the framework of a weakly coupled H-aggregate model [13], resulting from weak resonance-Coulomb coupling (J) of transition moments aligned cofacially in neighboring polymer chains [11]. In contrast, the absorption spectrum contains contributions from both the aggregate and nonaggregate regions [13]. From the ratio of the (0, 0) and (0, 1) absorbance peaks [14,15], we estimate a free-exciton bandwidth ($W = 4J$) of 100 ± 3 meV [13].

Figure 1(a) displays time-resolved PL measurements at 10 K. The PL spectrum decays substantially over subnanosecond time scales, and it redshifts by $>$40 meV with weak

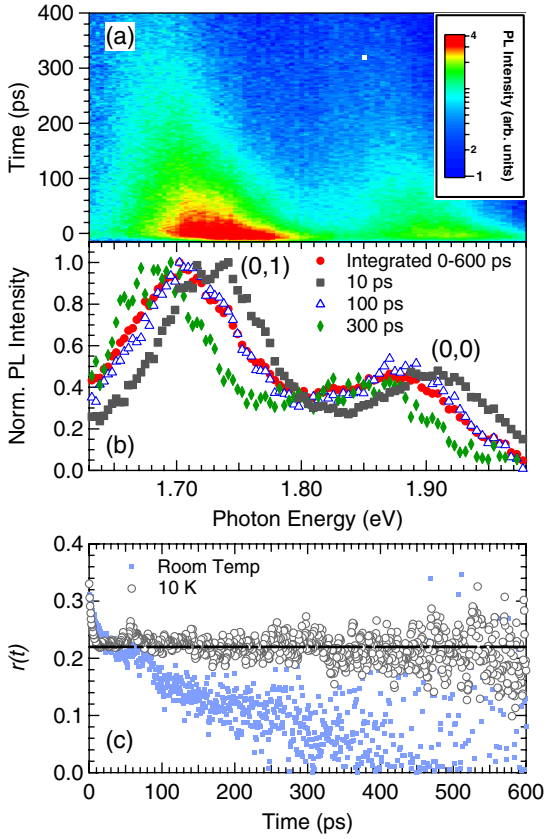

FIG. 1 (color online). (a) Time-resolved PL spectrum (10 K, 19 μJ cm^{-2} per pulse). (b) Normalized slices of (a) at various times. (c) Time-resolved PL anisotropy r at 10 K (open circles) and at room temperature (dots). The horizontal line indicates the average anisotropy between 20 and 600 ps.

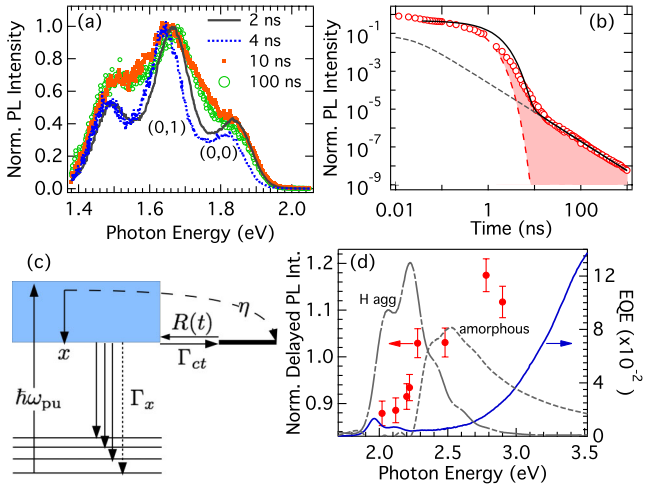

FIG. 2 (color online). (a) Time-resolved PL spectra at 10 K. (b) Spectrally integrated PL intensity versus gate delay. Data from Fig. 1 are included over subnanosecond time scales. The dashed lines represent a two-exponential fit with $\langle\tau\rangle = 235 \pm 23$ ps and an asymptotic power law $\{1/[1 + (t/\tau')^{\alpha}]\}$ with $\alpha = 1.54 \pm 0.08$ and $\tau' \ll \langle\tau\rangle$. A fit to the model [Eq. (1)], represented schematically in (c), is shown as a continuous line (for $\eta = 0.03$, $\Gamma_{CT} = 0.35$ ns^{-1}, $\Gamma_x = 1.23$ ns^{-1}, $\nu = 4.37 \times 10^{13}$ s^{-1}, $\mu = 0.54$). (d) Delayed PL excitation spectrum at 10 K, measured by phase-sensitive methods as described in the supplemental material [14], superimposed on the H-aggregate and -nonaggregate absorption spectra (see Ref. [15]). Also shown is the external quantum efficiency spectrum measured at 300 K in a ITO/PEDOT:PSS/P3HT/LiF/Al diode fabricated and encapsulated in a N_2-filled glove box.

evolution of the spectral band shape. We examine in more detail this spectral evolution in Fig. 1(b). Figure 1(c) displays the early-time PL anisotropy, defined as $r = (I_{\parallel} - I_{\perp})/(I_{\parallel} + 2I_{\perp})$, where $I_{\parallel(\perp)}$ is the instantaneous PL intensity parallel (perpendicular) to the linear polarization of the pump pulse. At 10 K (open circles), r decays to 0.22 ± 0.03 within the instrument response of several picoseconds due to exciton self-trapping in the photophysical aggregate [16,17], and does not evolve further on a subnanosecond window. In contrast, r decays to zero after 500 ps at room temperature. PL anisotropy decay is a signature of exciton diffusion [18], so at 10 K excitons are immobile over the time scale of the dynamic redshift in Fig. 1(a). Another possibility could be relaxation of excess vibrational energy following ultrafast excitation of the sample. Parkinson *et al.* reported that torsional relaxation of the backbone leads to more cofacial lamellar structures (more extended correlation of site energies in the aggregate [12]), leading to a dynamic loss of $(0, 0)$ intensity over $\sim$13 ps at 300 K [19]. We do not observe significant relaxation of the $(0, 0)$ relative intensity over the time scale of Fig. 1(a). Furthermore, upon increasing the temperature even slightly, the steady-state PL spectrum broadens significantly at 10 K [13], so we rule out thermal relaxation. We suggest that the dynamic spectral redshift of the PL spectrum results from an evolving electric field distribution [20] from photogenerated charges in the aggregate, which is consistent with charge photogeneration yields reported in the literature and our own transient absorption measurements [14]. If so, charges are generated over all time scales spanning $\lesssim 1$ ns, by a mechanism not involving exciton diffusion.

We next consider delayed PL dynamics due to charge recombination. Figure 2(a) displays time-gated PL spectra at 10 K. After a few nanoseconds, the aggregate spectrum is superimposed with a broader component (see Ref. [14]) with similar dynamics to those of the H aggregate since this composite band shape persists over microseconds. While we know that the aggregate spectrum arises from lamellar stacks, we conjecture that the featureless spectrum arises from nonaggregate regions. It is reminiscent of red-emitting species found in amorphous polymer films, often referred to as excimers [21]. From the delayed PL band shape in Fig. 2(a), we conclude that recombination occurs at the interface between H-aggregate and -nonaggregate regions, and can populate either species.

The total PL intensity decays exponentially over picosecond time scales, but asymptotically as a power law $[I(t) \propto t^{-1.54}]$ for times much longer than the exciton lifetime [Fig. 2(b)]. This behavior can arise from unimolecular

charge recombination [22] or by triplet bimolecular annihilation [23,24]. We find that the delayed PL intensity varies linearly with the pump fluence [14], which permits us to assign the power-law decay to exciton regeneration by charge recombination with a distribution of rates, as the other two possibilities would lead to a nonlinear fluence dependence. The power-law decay is independent of temperature [14], suggesting recombination by tunneling. We note that we cannot reproduce the measured time-resolved PL intensity as a simple superposition of a multiexponential and an asymptotic power-law decay, as the time window spanning 1–10 ns features a PL decay over nearly 3 orders of magnitude that deviates significantly from either decay function [Fig. 2(b)]. This indicates that the two PL decay phenomena are not independent, but that one decay regime evolves into the other, with competing kinetics on nanosecond time scales. By integrating the PL intensity over time scales where the decay is nonexponential, we find that $\geq 12\%$ of the time-integrated intensity is accounted for by slow recombination. This reflects a significant density of charge pairs.

Based on the results of Figs. 1 and 2 and building upon previous reports [5–9], we construct the following photophysical picture, depicted schematically in Fig. 2(c). Upon photoexcitation, charge pairs are generated with efficiency η, and the rest of the population relaxes to self-trapped excitons x in <1 ps [17]. These decay to the ground state with rate constant Γ_x or charge separate with rate constant Γ_{CT}. Charge pairs may recombine to regenerate x with a temporal distribution $R(t)$. Thus,

$$\frac{dx}{dt} = -(\Gamma_x + \Gamma_{\mathrm{CT}})x + \eta R(t) + \int_0^t \Gamma_{\mathrm{CT}} x(t') R(t - t') dt'. \tag{1}$$

Assume a distribution of charge-pair distances $f(r) = \epsilon e^{-\epsilon r}$. The tunneling rate is $k(r) = \nu e^{-\beta r}$ and its time distribution is $R(t) = \int_0^\infty f(r) k(r) e^{-k(r)t} dr$. With $x(0) = 1 - \eta$, the Laplace transform of Eq. (1) is

$$\hat{x}(s) = \frac{1 - \eta + \eta \hat{R}(s)}{s + \Gamma_x + \Gamma_{\mathrm{CT}}[1 - \hat{R}(s)]}, \tag{2}$$

where $\hat{R}(s) = \mu \int_0^\infty e^{-(1+\mu)\chi}/(s/\nu + e^{-\chi}) d\chi$, $\chi = \beta r$, and $\mu = \epsilon/\beta$. The model predicts biphasic dynamics with PL intensity, $I(t) \propto \Gamma_x x(t)$, evolving as $I(t) \propto \exp(-\Gamma_x t)$ at short times and as $I(t) \propto t^{-(1+\mu)}$ at long times. We evaluate Eq. (2) as described elsewhere to recover $I(t)$ [25].

The most robust parameter in this model is the ratio of the characteristic electron-hole separation (ϵ) and the distance dependence of charge tunneling (β): $\mu = \epsilon/\beta = 0.54 \pm 0.08$, as it defines uniquely the slope of the power-law decay at long times. Hence, $\epsilon \approx 0.54\beta$; a significant fraction of charge pairs do not recombine in the microsecond time scale, as the tail of $f(r)$ extends beyond the characteristic length scale of $k(r)$. The charge-pair population is expected to survive on much longer time scales, which is consistent with reports of a high residual charge density in P3HT at steady state [26,27].

We next consider η. We cannot extract it uniquely from the model, as it is coupled to Γ_{CT}. Both parameters affect the amplitude of the power-law decay without altering the decay rate. We probe the range of η that is consistent with the literature, and explore the consequences on Γ_{CT}. With $\Gamma_x = 1.23$ ns^{-1} [fixed by the slow part of the biexponential decay in Fig. 1(a)] and with $\nu = 4.37 \times 10^{13}$ s^{-1} (corresponding to the frequency of the aromatic *C*-*C* stretch measured by Raman spectroscopy [28]), we find that if we set $\eta = 3\%$, we require $\Gamma_{\mathrm{CT}} = 0.35 \pm 0.05$ ns^{-1}, but if $\eta = 30\%$ we can reproduce the data with $\Gamma_{\mathrm{CT}} = 0$. With $\eta = 40\%$, we can no longer obtain a satisfactory fit of the amplitude of the power-law component, which is overestimated. We have interpreted the dynamic redshift of the PL spectrum (Fig. 1) as a consequence of an evolving electric field on the subnanosecond time scale, which is comparable to the exciton lifetime. In order to rationalize our time-resolved spectroscopic data, we therefore consider that $\Gamma_{\mathrm{CT}} \lesssim \Gamma_x$, which from the modeling would imply that $\eta < 10\%$ in the solid-state microstructure of our films.

If the two slow-decaying emissive species in Fig. 2(a) are due to regeneration of aggregate and nonaggregate excitations by charge tunneling, we propose that charges are initially generated at the interface between the two domains. To explore this further, we have carried out quantum-chemical calculations [29] on a stack of ten oligothiophene chains [Fig. 3(a)] to represent the crystalline moieties in the higher molecular weight (i.e., longer chain) P3HT used in our experimental study. We note higher conformational disorder at the top and bottom of the stack, leading to a higher excitation energy in those regions compared to the center [Fig. 3(b)]. Figure 3(c) displays the calculated absorption spectrum in a given configuration. For all stack configurations studied, we always observe a shoulder at $\sim$2.7 eV on the blue side of the main absorption band at $\sim$2.4 eV. (Note that these energies are overestimated, but the $\sim$0.3 eV difference is meaningful.) The excited states that are generated in this spectral region are quasidegenerate with the lowest-lying charge-transfer (CT) states, shown by the superimposed plot of CT character as a function of excitation energy. We can identify three regimes of the spatial distribution of transition densities, shown in Fig. 3(d). The excitation with the lowest transition energy (I) is always confined to the center of the stack over 2–3 sites as a result of disorder and is weakly emissive (H aggregate); the intermediate excitation (II) carries most of the oscillator strength and is delocalized in the center of the stack; the higher-lying excitation (III) is dominated by conformationally disordered chains at the ends of the stack, but it communicates with chains in the center so that charge separation of these higher-energy states is possible. In our measurements, we excite $\sim$0.3 eV above the (0, 0) absorption, placing us at the limit of CT excitation predicted by Fig. 3(c). We have measured the delayed PL excitation spectrum, shown in Fig. 2(d).

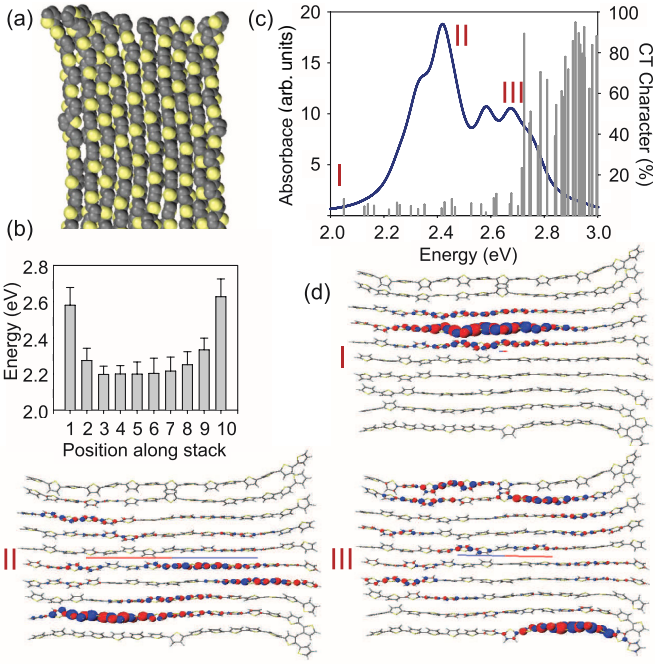

FIG. 3 (color online). (a) Snapshot of an aggregate architecture (15-mers in a 10-chain stack [29]). (b) Average site excitation energy (uncertainty is the variance), averaged over many excited-state calculations on isolated conformers extracted from the stack. (c) Absorption spectrum for one configuration of the full stack superimposed to the corresponding CT character. (d) Transition densities (ground-state—excited-state overlap) for excitations of increasing energy.

This reveals that excitation on the edge of the component of the absorption spectrum due to less ordered or amorphous species enhances the delayed PL yield, consistent with the significant CT character of excitons at these photon energies. Photocurrent measurements reveal that a further 0.4-eV energy is required to produce charge carriers [Fig. 2(d)], underlining that our delayed PL measurements probe recombination of tightly bound geminate polaron pairs (not carriers) produced by excitation with energies $\lesssim 3$ eV. Deibel *et al.* reported that 0.42-eV excess energy above the optical gap is required to produce polaron pairs, and then a further 0.3 eV to generate photocarriers [10], consistent with our findings.

We have presented compelling evidence that excitons with sufficient energy dissociate *extrinsically* near interfaces between molecularly organized and less organized domains, underlining the importance of the disordered energy landscape. This competes with dissociation at heterojunctions in photovoltaic diodes [1].

C. S. acknowledges NSERC and the CRC in Organic Semiconductor Materials. G. L. and N. S. acknowledge the EC 7th Framework Program ONE-P project (Grant Agreement 212311). D. B. is also partly supported by ONE-P (NMP3-LA-2008-212311), the Interuniversity Attraction Pole IAP 6/27 of the Belgian Federal Government, and FNRS/FRFC. P. L. K. thanks FQRNT, and M. S. thanks MELS/FQRNT.

*Current address: Centre for Biomolecular Nanotechnologies, Italian Institute of Technology, Lecce, Italy.
†carlos.silva@umontreal.ca

[1] See T. M. Clarke and J. R. Durrant, Chem. Rev. **110**, 6736 (2010) for a comprehensive review.
[2] H. Sirringhaus *et al.*, Nature (London) **401**, 685 (1999).
[3] F. C. Spano, Annu. Rev. Phys. Chem., **57**, 217 (2006).
[4] C. Silva *et al.*, J. Phys. Condens. Matter, **14**, 9803 (2002).
[5] E. Hendry *et al.*, Phys. Rev. Lett., **92**, 196601 (2004).
[6] X. Ai *et al.*, J. Phys. Chem. B **110**, 25462 (2006).
[7] C. Sheng *et al.*, Phys. Rev. B **75**, 085206 (2007).
[8] P. D. Cunningham and L. M. Hayden, J. Phys. Chem. C **112**, 7928 (2008).
[9] J. Piris *et al.*, J. Phys. Chem. C **113**, 14 500 (2009).
[10] C. Deibel *et al.*, Phys. Rev. B **81**, 085202 (2010).
[11] F. C. Spano, J. Chem. Phys. **122**, 234701 (2005); **126**, 159901 (2007)
[12] F. C. Spano *et al.*, J. Chem. Phys. **130**, 074904 (2009).
[13] J. Clark *et al.*, Phys. Rev. Lett. **98**, 206406 (2007).
[14] See supplemental material at http://link.aps.org/supplemental/10.1103/PhysRevLett.106.197401 for further time-resolved PL and transient absorption measurements.
[15] J. Clark *et al.*, Appl. Phys. Lett. **94**, 163306 (2009).
[16] M. H. Chang *et al.*, Phys. Rev. Lett. **98**, 027402 (2007).
[17] E. Collini and G. D. Scholes, Science **323**, 369 (2009).
[18] We excite both H aggregates and nonaggregates with similar probability at 2.33 eV [14], so exciton diffusion would result in a dynamic memory loss of the ensemble-average transition-dipole-moment orientation. We observe this at 300 K because exciton diffusion is thermally activated, but not at 10 K. See D. Beljonne *et al.*, J. Phys. Chem. B **109**, 10594 (2005) for relevant modeling.
[19] P. Parkinson *et al.*, J. Phys. Chem. Lett. **1**, 2788 (2010).
[20] R. Kersting *et al.*, Phys. Rev. Lett. **73**, 1440 (1994).
[21] B. J. Schwartz, Annu. Rev. Phys. Chem. **54**, 141 (2003).
[22] B. Schweitzer *et al.*, Chem. Phys. Lett. **313**, 57 (1999).
[23] A. Gerhard and H. Bässler, J. Chem. Phys. **117**, 7350 (2002).
[24] C. Rothe and A. Monkman, J. Chem. Phys. **123**, 244904 (2005).
[25] C.-N. Brosseau *et al.*, Phys. Rev. B **82**, 085305 (2010).
[26] G. Dicker, M. P. de Haas, and L. D. A. Siebbeles, Phys. Rev. B **71**, 155204 (2005).
[27] A. J. Ferguson *et al.*, J. Phys. Chem. C **112**, 9865 (2008).
[28] Y. Gao *et al.*, J. Phys. Chem. Lett. **1**, 178 (2010).
[29] Semiempirical INDO/SCI excited-state calculations (including 200 molecular orbitals in the active space) have been performed on the basis of snapshots extracted from molecular dynamics simulations of the stack, using a force field parametrized against high-level *ab initio* calculations. Further details will be reported elsewhere.